



The Samos Mw6.9 event: Damage investigation in the town of Vathy incorporating a stochastic finite-fault source with site and structural information

Georgia Giannaraki^{1,2}, Zafeiria Roumelioti¹, and Nikolaos S. Melis²

¹University Of Patras, Department Of Geology, Patras-Greece

²National Observatory Of Athens, Institute Of Geodynamics, Athens-Greece

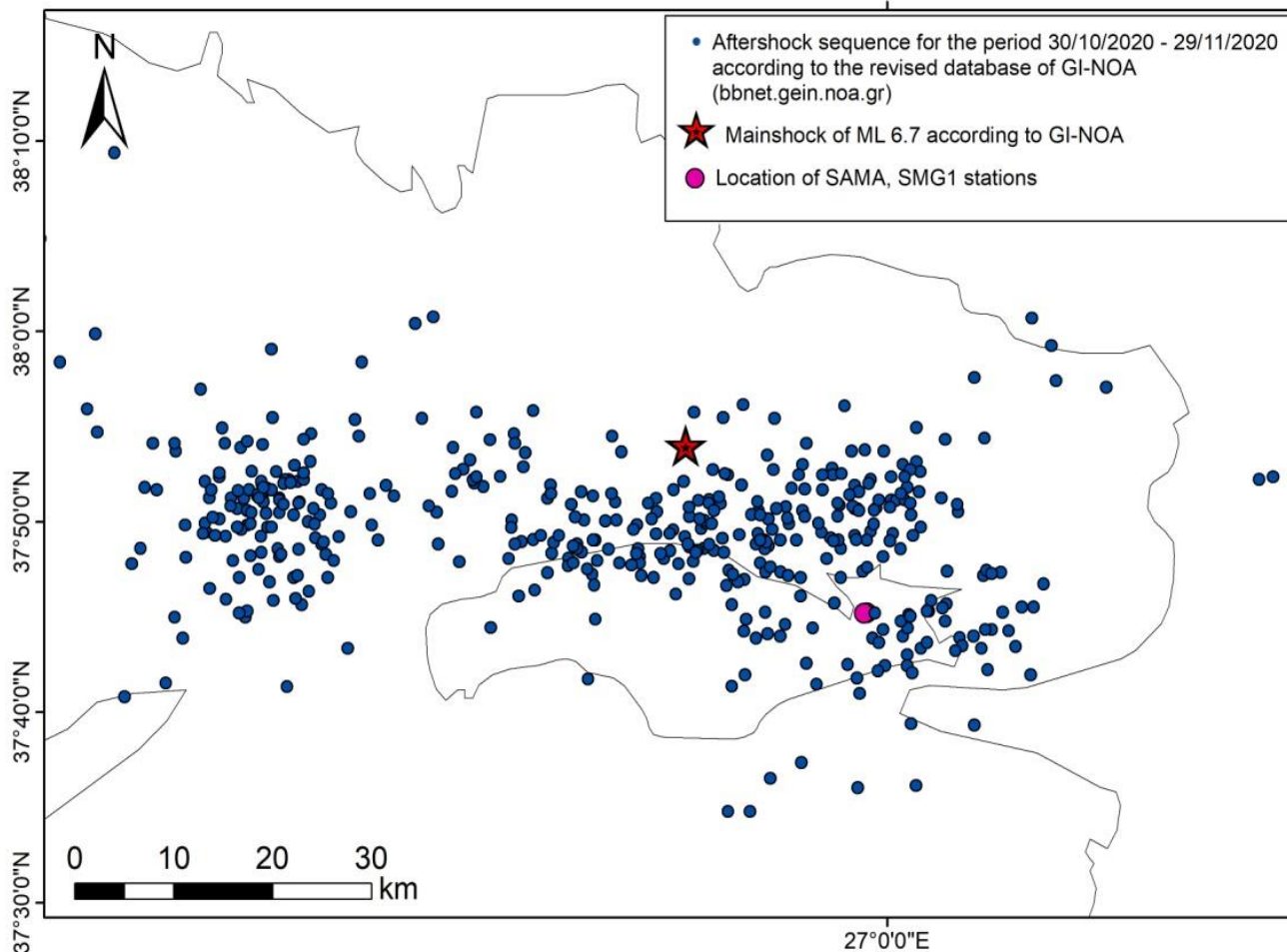
Purpose of the research

To reproduce the damage distribution pattern in Vathy, the capital of Samos island, caused by the M7.0 October 30, 2020 earthquake

To this aim:

- 1) We computed the input PGA field throughout the area covered by the building stock of Vathy (stochastic method, EXSIM code)
- 2) We included site effects by compiling a proxy ($V_{S,30}$) map and assigning empirical amplification factors
- 3) We incorporated structural vulnerability and performed risk assessment in terms of EMS-98 Damage Grades

Finite Fault modelling of the M7.0 Samos event



Samos 2020 seismic sequence for a period of 1 month

Most preliminary source studies agree on that the aftershocks of the 2020 sequence are distributed across a much wider area than the one that ruptured during the **M7.0** earthquake



The location and dimensions of the seismogenic source are still debating issues

Investigating the Optimum Location for the Adopted Fault Plane

Constrained:

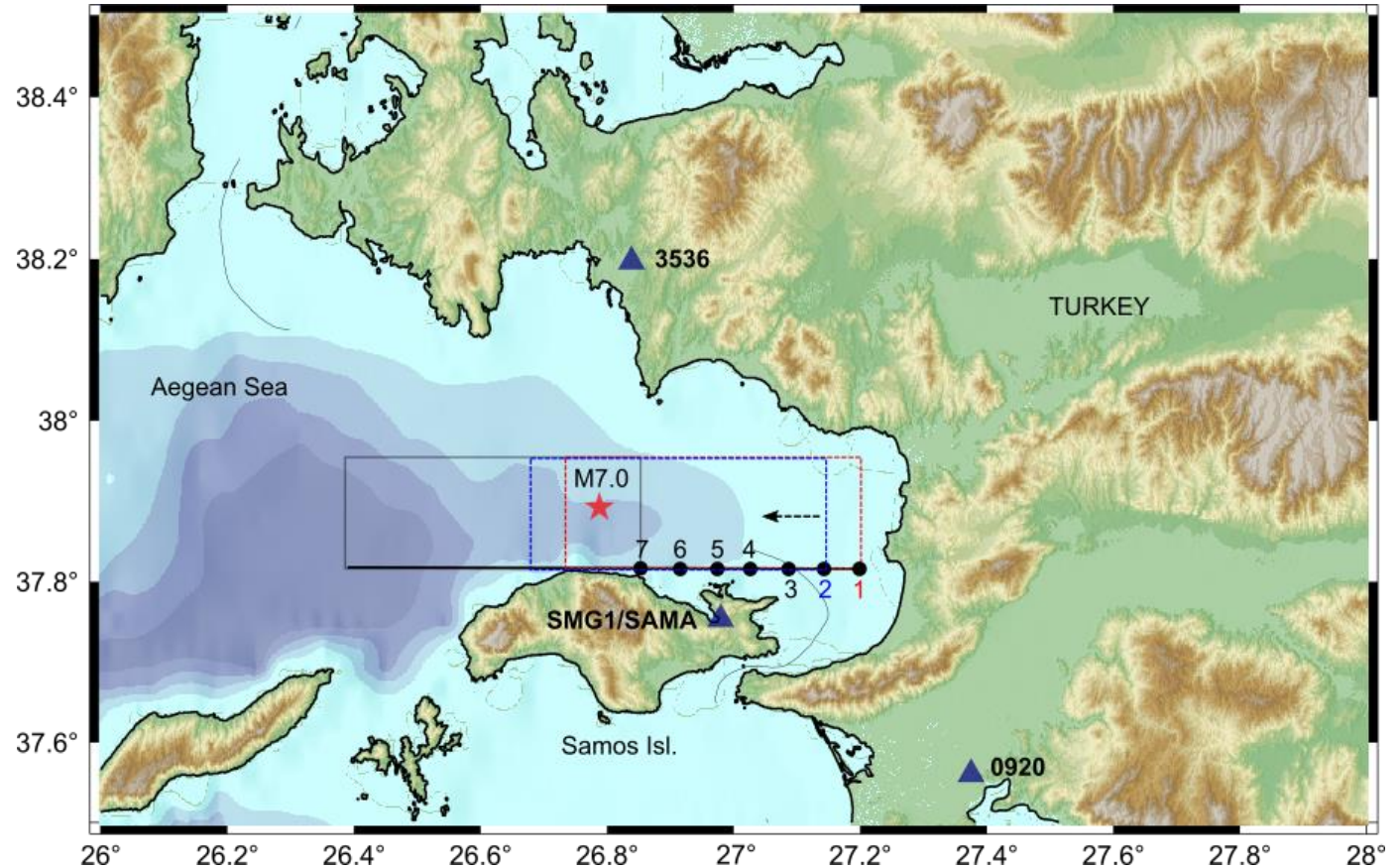
- Fault plane dimensions (42x20 km, empirical, Wells and Coppersmith 1994)
- Rupture mechanism (GCMT solution)
- Epicenter (Plicka et al., 2021)

Tested:

7 different positions starting from the East (point 1) and gradually shifting (by 5 km) the fault plane to the West (westernmost position at point 7)

Evaluation Criterion:

Model bias: mean \log_{10} ratio of synthetic-to-observed Fourier Amplitude Spectra ($FAS_{\text{synt}}/FAS_{\text{obs}}$) at the two closest rock stations (AFAD Stations 3536 and 0920)* (<https://tadas.afad.gov.tr>)



Depiction of different tested positions of upper edge of fault

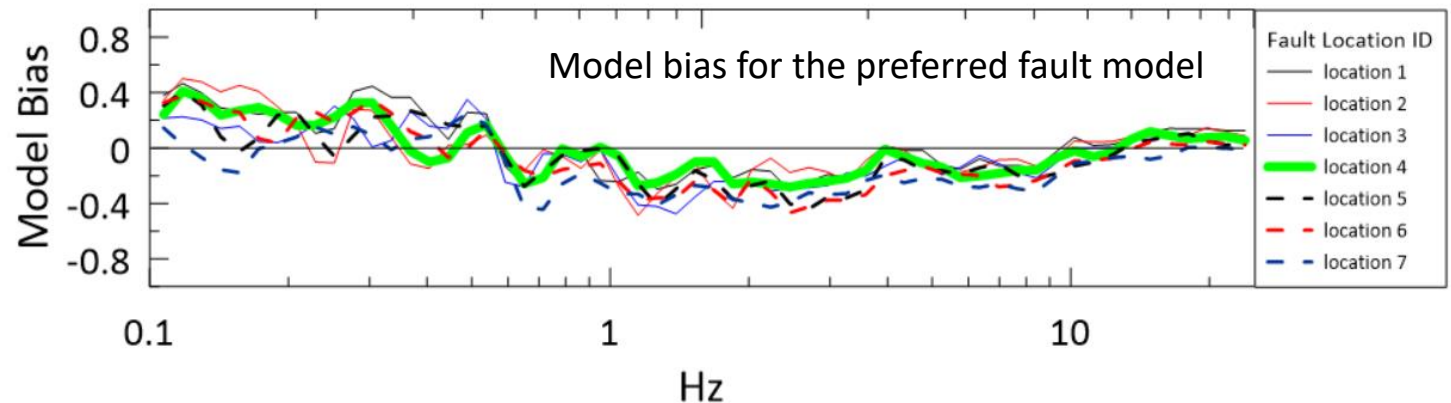
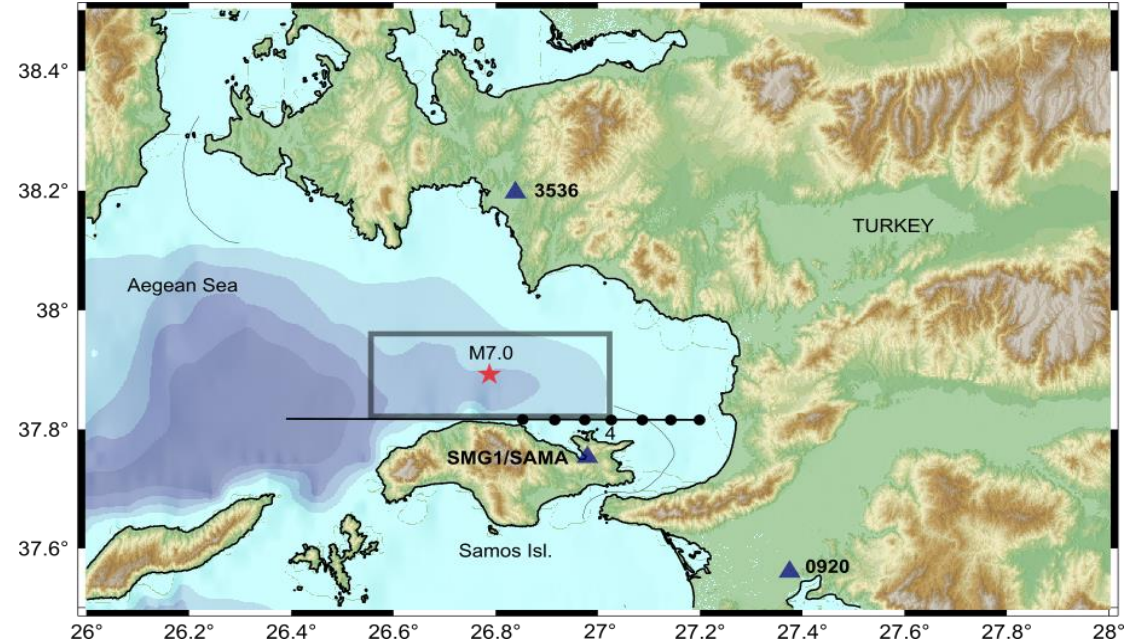
*SAMA, although a “rock” station, was not involved in this stage due to its low resolution and because it is installed at the basement of a 3-story building (possible Soil-Structure-Interaction contamination)

Defining the Optimum Location for the Adopted Fault Plane

Best fitting model corresponds to **fault location id 04**: model bias is closer to zero throughout most of the examined frequency range, especially in the intermediate-high frequencies where PGA (our target ground motion measure) is expected

In general, western locations (dashed curves) perform better at low frequencies (<0.55Hz) and eastern locations at higher frequencies (>0.55Hz)

Preferred location of the adopted fault model

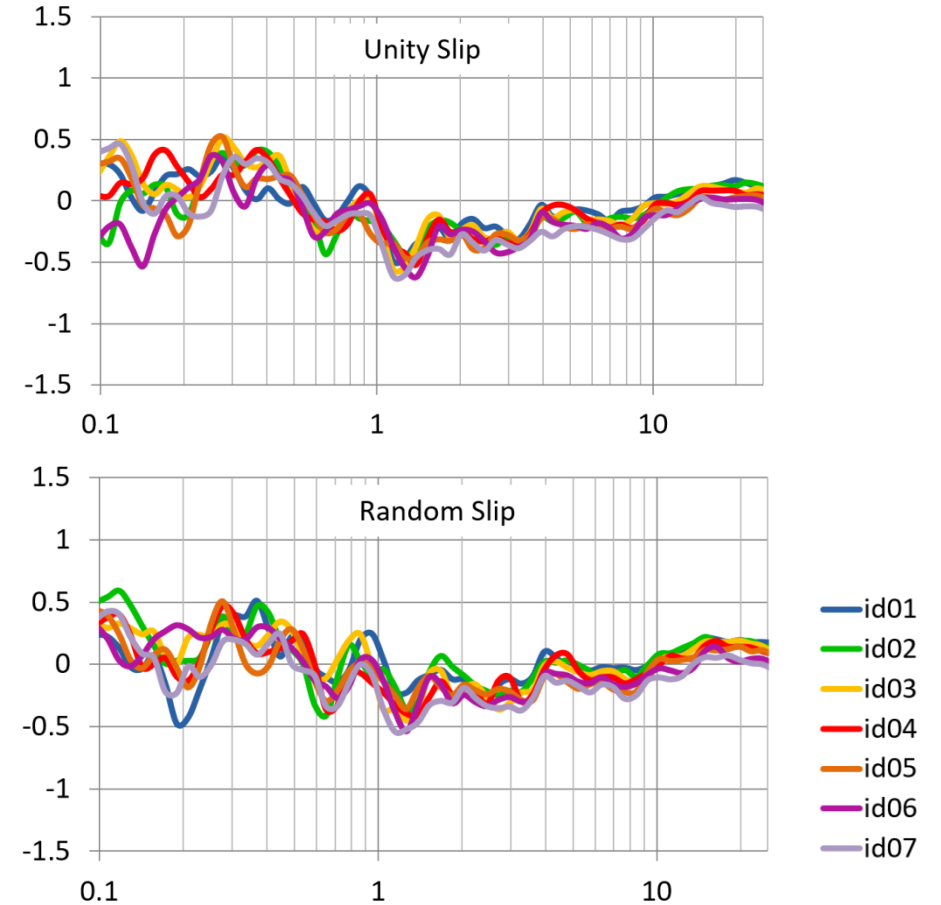
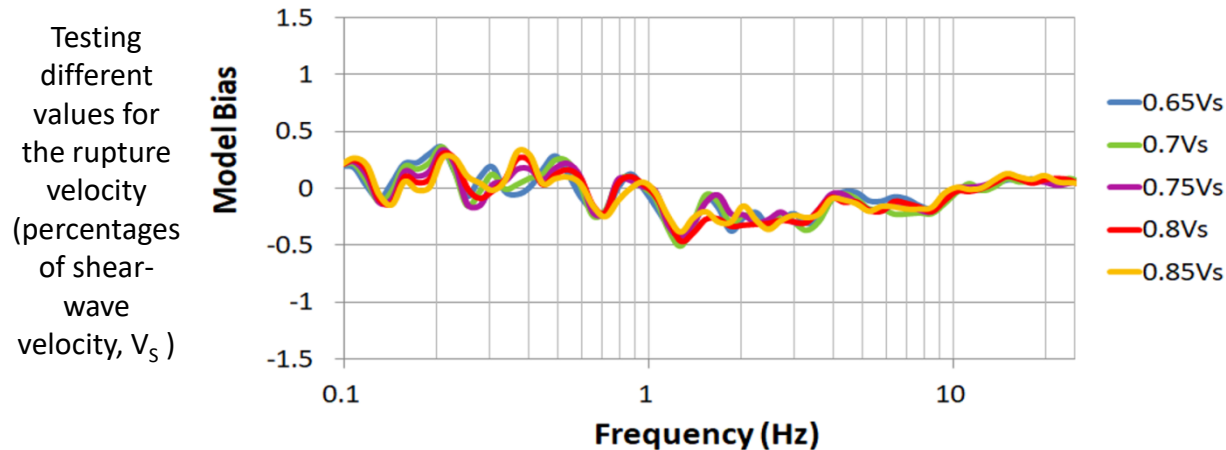


Calibrating the Stochastic Model

We tested different parameters of the stochastic model toward improving the fit of PGA, acceleration waveform envelopes and FAS of the two AFAD rock stations, including:

- The stress parameter
- The pulsing percentage
- Unity slip against random slip
- Rupture velocity

Overall, the model did not present statistically significant sensitivity in any of these parameters, at least for the two studied stations

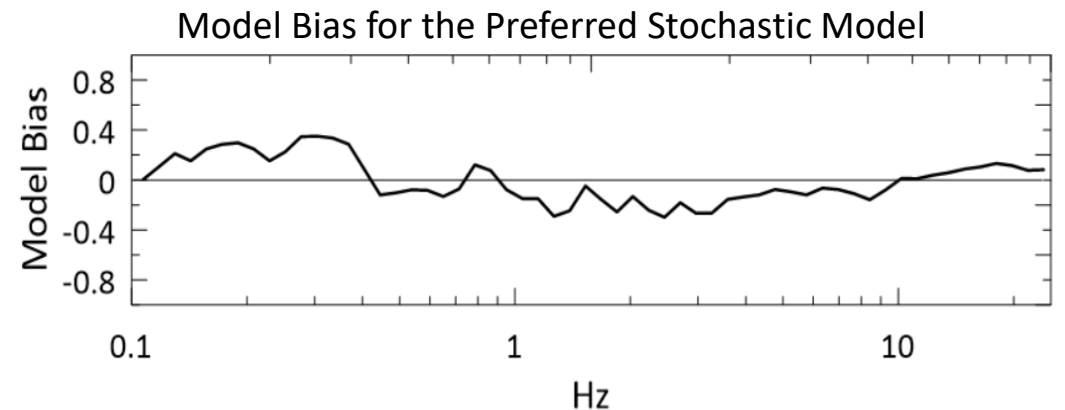


Comparison of the model bias for unity and random slip for the different trial positions of the fault plane

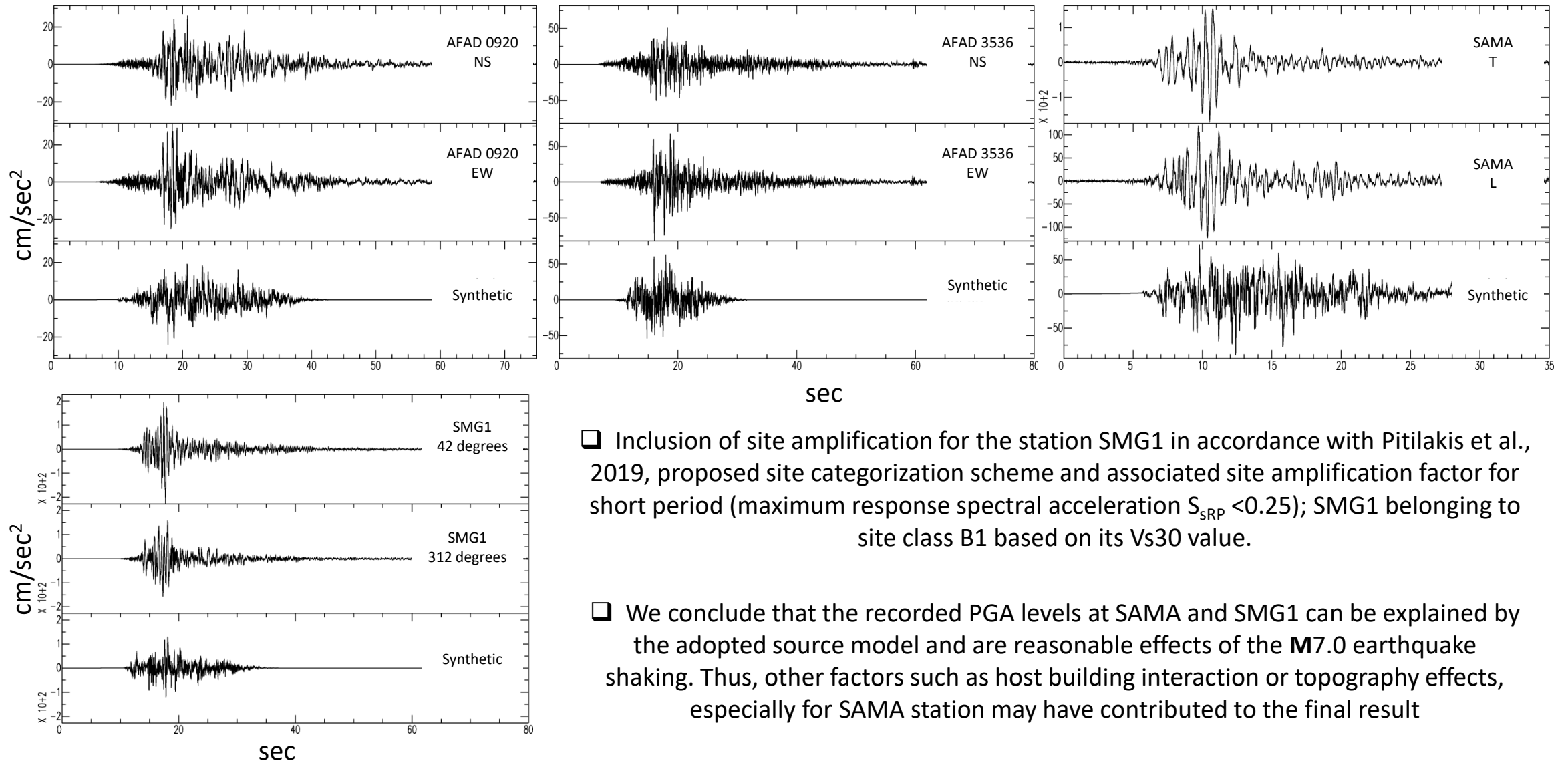
Parameters of the final (preferred) model used to simulate the PGA field in Vathy

Basic Input parameters employed in the stochastic simulation	Value / reference
Adopted Epicenter	Plicka et al., 2021
Mw	7.0
Strike (°), dip (°), rake (°), Type of Fault	276, 34, -95, Normal (according to GCMT)
Fault Length x Width (km), Depth of upper edge of fault (km)	40 x 20, 2
Subfault dimensions dl x dw (km)	5 x 5
Hypo location in along fault and down dip distance (km)	4, 12
Type of slip	Trimmed version of Kiratzi A. (pers. comm.)
Stress parameter (bars)	56 (Margaris and Boore, 1998)
Anelastic attenuation model Q(f) Q(f) = $Q_0 \cdot (f)^n$, $f \leq 0.2$ Q(f) = $Q_0 \cdot (f)^n$, $f \geq 0.6$	275, -2.0 88, 0.9 Q determined from a power law fit for $0.2 < f < 0.6$ (Boore, 1984, 1996, 2005; Hatzidimitriou, 1993, 1995; Margaris and Boore, 1998)
Geometric Spreading as a function of distance (km)	R^{-1} from 1.0 to 70 km R^0 from 70 to 130 km $R^{-0.5}$ beyond 130 km (Atkinson and Mereu, 1992; Atkinson and Boore, 1995, Boore, 2005; Hatzidimitriou, 1993, 1995; Margaris and Boore, 1998)

Basic Input parameters employed in the stochastic simulation	Value / reference
Windowing function	Exponential of taper 0.05 (Boore, 2005)
Kappa (sec)	0.035 for rock site simulation according to Margaris and Boore, 1998
Crustal shear-wave velocity (km/sec)	3.4
Ruprure Velocity (km/sec)	2.72 [= 0.8 · (shear-wave velocity)]
Crustal density at source depth (gr/cm ³)	2.7



Observed vs Synthetic acceleration time histories for the adopted final stochastic model at rock site stations (top) and SMG1 station (bottom)



□ Inclusion of site amplification for the station SMG1 in accordance with Pitilakis et al., 2019, proposed site categorization scheme and associated site amplification factor for short period (maximum response spectral acceleration $S_{SRP} < 0.25$); SMG1 belonging to site class B1 based on its V_{s30} value.

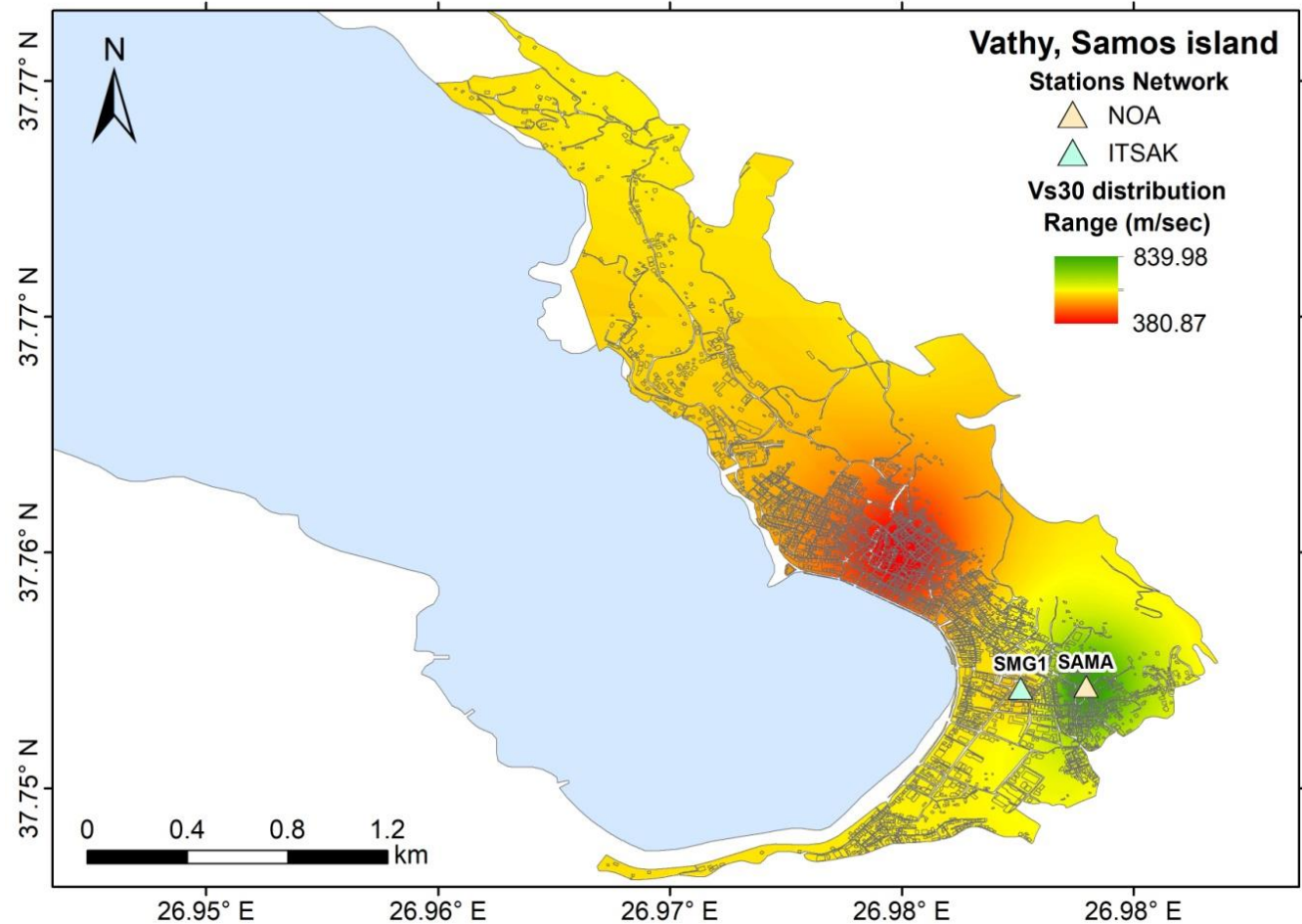
□ We conclude that the recorded PGA levels at SAMA and SMG1 can be explained by the adopted source model and are reasonable effects of the **M7.0** earthquake shaking. Thus, other factors such as host building interaction or topography effects, especially for SAMA station may have contributed to the final result

$V_{S,30}$ Map for Vathy

$V_{S,30}$ distribution in Vathy was determined based on local geology, terrain-based proxies according to Stewart et al., 2014, and the $V_{S,30}$ measurements at the sites of the two permanent accelerometric stations in the town of Vathy

Higher $V_{S,30}$ values are attributed to the south-central part of Vathy, in the area towards the port of the town

Site effect has been considered by attributing a **mean value of $V_{S,30}$ per building block** and a corresponding site class according to Pitilakis et al. (2019) and additional geotechnical information provided in the GEER-069 report (2020)

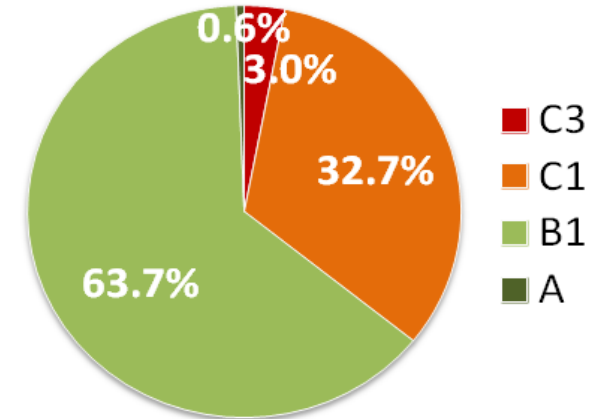


Soil Classification for Incorporating Site Effects

Vs30 * (m/sec)	Soil Class	Soil Description	Site Amplification Factor for short period and $SsRP^* < 0.25$
[385-400)	C3	Medium dense sand and gravels and/or medium stiffness clays of great thickness.	1.8
[400-500)	C1	Dense sand and gravels and/or stiff clays, of great thickness	1.7
[500-800)	B1	Soft Rock	1.3
≥ 800	A	Rock	1

* The range of Vs30 and the respective soil class is attributed in this way for higher safety

* SsRP = The reference maximum spectral acceleration, corresponding to the constant acceleration branch of the horizontal 5% damped elastic response spectrum on site class A

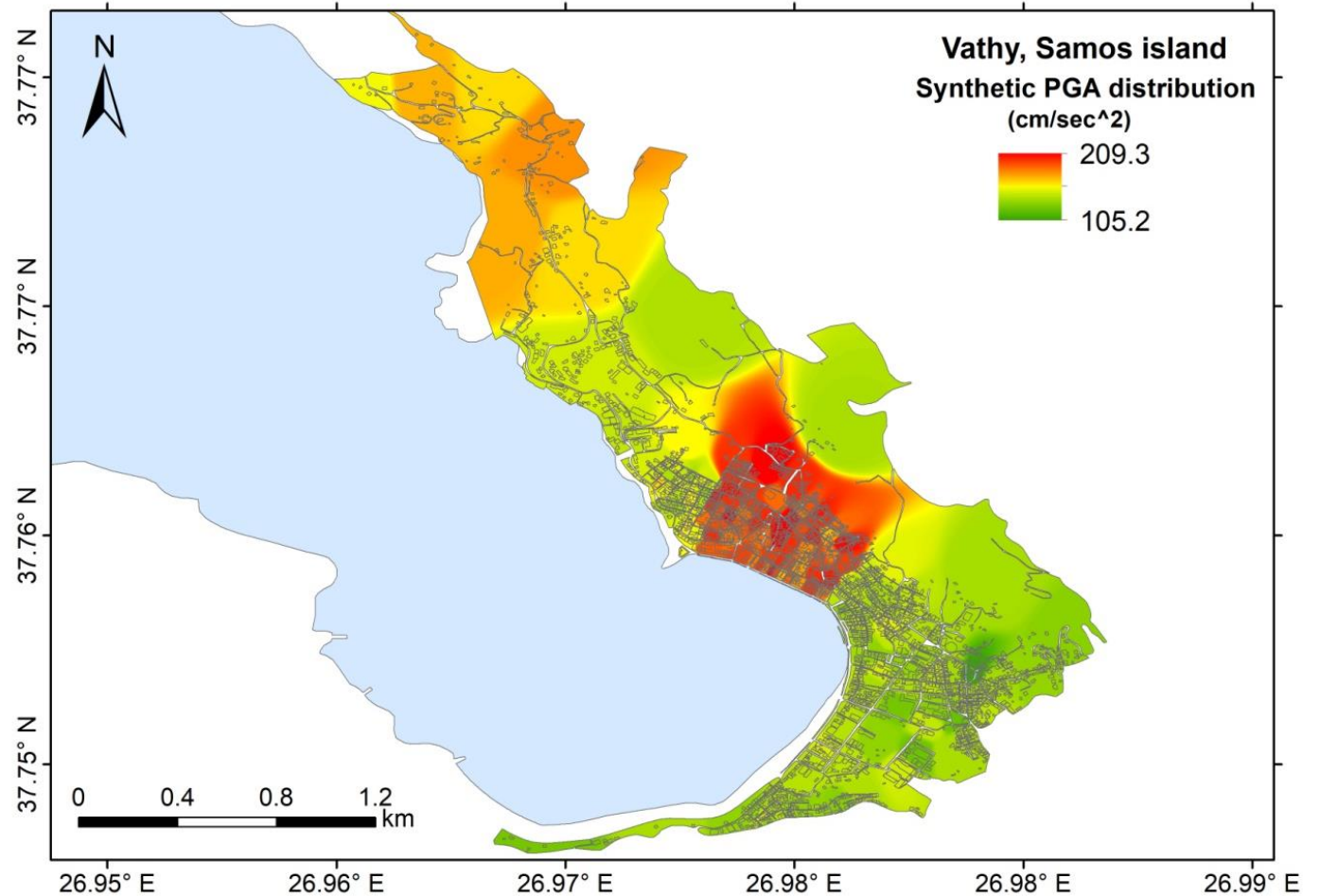


The percentage of building blocks in Vathy with the assigned respective Soil Class

Synthetic PGA distribution in Vathy; Site Effects Included

The synthetic for “rock” site conditions PGA values (average of 10 simulations at each grid point) were appropriately amplified based on the previously presented soil classification and empirical amplification factors

Higher PGA values have been computed in the central part of Vathy (softer soil) and in the northern part (closest to the source)





Seismic vulnerability in Vathy is assessed taking into consideration the empirical RiskUE-LM1 approach as proposed by Giovinazzi and Lagomarsino, 2004. The exposure model of the town is based on available census data (EPANTYK, 2009) which contains information of the town's building stock per inspected building, at a block-by-block level, regarding:

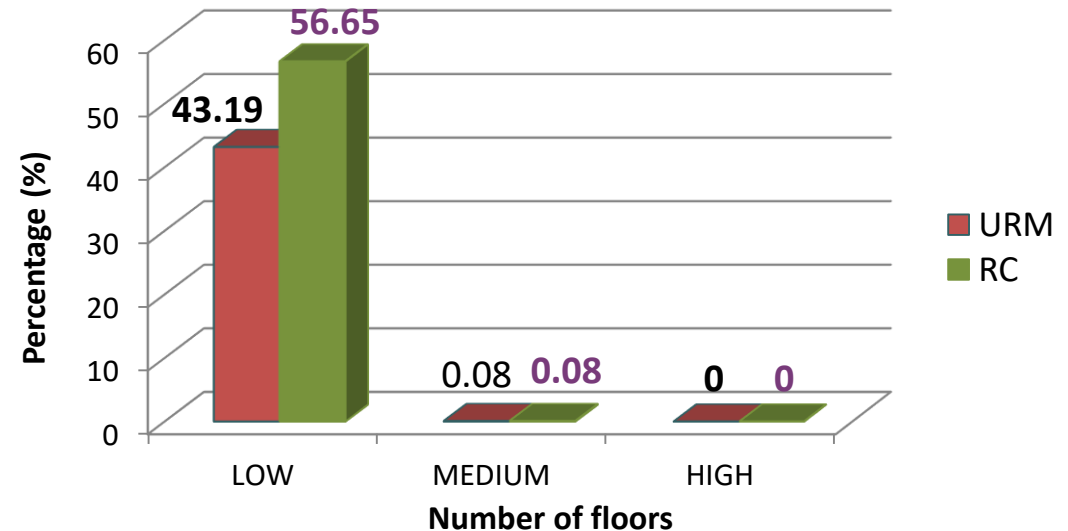
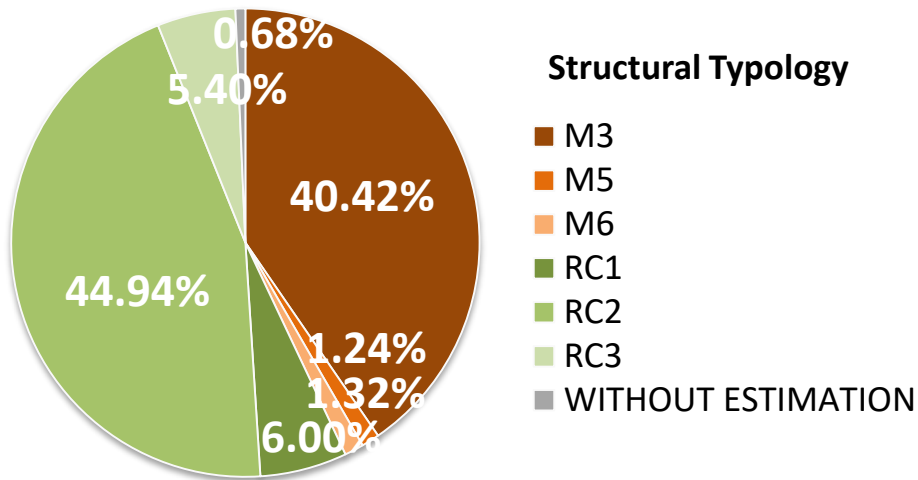
- The census building block code to which the inspected building belongs, while the exact position of the building inside its respective block is not specified due to reasons of personal data retention.
- The number of floors
- The period of construction
- The construction material
- The existence of basement, ground floor, pilotis
- Roofing materials
- Exclusive and/or mixed; main and secondary, use of the building

In the present analysis, infrastructures that have not been recorded with a specific definition of construction material (probably mixed constructions in terms of material), Reinforced Concrete (**RC**)/béton and UnReinforced Masonry (**URM**) buildings of bricks/cement blocks for which the period of construction is not specified are omitted due to unavailable classification of the Typological Vulnerability Index (V_1^*). Timber typologies according to the census; a percentage of 0.24% of the total, are additionally excluded from the elaboration of the dataset since the adopted methodology approach mainly concerns URM and RC Typologies.

Defining the Exposure

The final exposure sample considered for the vulnerability analysis consists of 2.482 buildings, both residential and public use, corresponding to 153 building blocks, out of which 6 building Typologies are classified with respect to the available census description of structural characteristics:

- 3 types of URM (43.27%); **M3**: Simple stone, **M5**: Unreinforced masonry/old bricks, **M6**: Unreinforced masonry/bricks with RC floors → M6 Typology is considered herein to be corresponded after the year 1970 as newer constructions of masonry
- 3 types of RC frames (56.73%), been classified in agreement with the evolution of the Greek Seismic Design Codes; **RC1**: Frame in RC without Earthquake Resistant Design/ERD, **RC2**: Frame in RC with moderate ERD, **RC3**: Frame in RC with high ERD



Percentages of URM, RC and undefined building Typologies in Vathy (left) and percentages in the final sample reflecting the number of floors

Assigning Vulnerability

Behavior Modifiers	Attributes	Census coding of period of construction	URM		RC			
		1: < 1919	M3 ⁽¹⁾	M5		RC1		
		2: 1919 – 1945						
		3: 1946 – 1960		M6		RC2		
		4: 1961 – 1970						
		5: 1971 – 1980						
		6: 1981 – 1985						
		7: 1986 – 1990						
		8: 1991 – 1995						
		9: > 1996						
10: Under construction (>2001)					RC3			
		V_i^*						
		0.74	0.616	0.644	0.484	0.324		
		Most Probable VC per EMS-98 (Grünthal, 1998)						
		B	C		D	E		
		V_{mk}						
Number of floors	Low: [0-2] ^a ; [0-3] ^b	-0.04		-0.02				
	Medium: [3-5] ^a ; [4-7] ^b	0						
	High: $\geq 6^a$; $\geq 8^b$	0.04	0.08		0.06	0.04		
Vertical Irregularity (Geometry/Mass distribution)	Existence of basement	0.04						
	Mixed use ⁽¹⁾							
	Existence of pilotis		0.04	0.02	0			
Roof (Weight, thrust connections)	Existence of concrete roof	0.04	0					
Aggregate Building position	Adjacent to neighboring buildings ⁽²⁾	0.06						
	Adjacent/Insufficient aseismic joints			0.04	0			

Building Typologies in Vathy with the adopted Typological Vulnerability Index and scores for structural Behavior Modifier factors, with the most probable Vulnerability Class (VC) per EMS-98 been further attributed:

Seismic Behavior Modifiers (ΔV_m) and their corresponding empirical scores (V_{mk}) according to Giovinazzi and Lagomarsino (2004) are additionally attributed to each certain building Typology after the assignment of the most probable Typological Vulnerability Index V_i^* accounting for structural and morphological peculiarities that can be deduced from the description of the available census dataset, according to the Table on the left.

⁽¹⁾Mixed use of buildings has been included to Vertical Irregularity for higher safety as this may indicate, e.g., the existence of department stores and therefore, the discontinuity of floors.

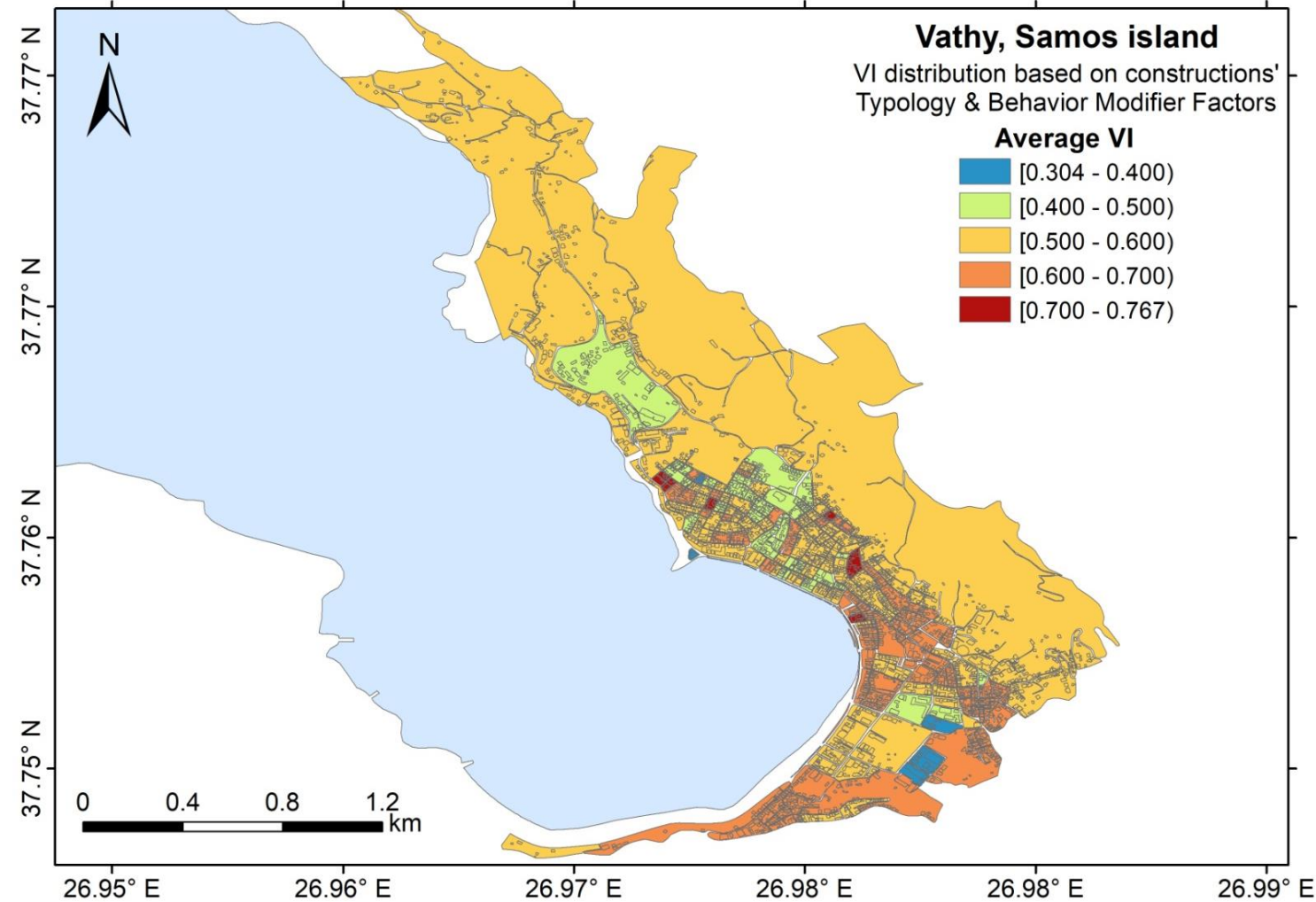
⁽²⁾Since the information of whether a building is adjacent to its neighboring buildings is available to the census dataset but not its exact position about how it is adjacent to them, the aggregate position of header is considered in the case of URM buildings for higher safety.

⁽³⁾The code characterization of simple stone exists in the census dataset, therefore, the type M3 is considered in these cases of category description for higher safety.

^a URM, ^b RC

Vulnerability Map of Vathy

Total Vulnerability Index VI was computed according to the equation of Giovinazzi and Lagomarsino (2004), where r_k is the ratio of building affected by the behavior modifier k characterized by the V_{mk} behavior score. The average value \bar{V}_I per building block was defined.



$$\bar{V}_I = V_I^* + \Delta V_m \rightarrow$$

$$\bar{V}_I = V_I^* + \sum_k r_k * V_{mk}$$

Higher structural vulnerability appears in the southwest part of the town, especially in the waterfront area and near to the port, where several low-rise old URM structures are located

Distribution of the estimated average Total VI in the town of Vathy based on constructions Typology and Behavior Modifier Factors as it is exported from the available census data and after the inclusion of further 12 building blocks with missing data; via the adoption Aerial geostatistical interpolation method (<https://desktop.arcgis.com>)

Damage estimation in Vathy

Seismic risk is finally assessed per building block by combining the simulated PGA wavefield, including site effects, and the structural vulnerability model

Modified Mercalli Intensity MMI values per building block, as a function of the respective synthetic PGA, were computed from (Tselentis and Danciu, 2008) :

$$MMI = 3.563 \cdot \log (PGA) - 0.946$$

Derived values range between 6.2 and 7.3, in accordance with corresponding macroseismic observations in Vathy (e.g., <https://www.emsc-csem.org/>, GEER Report).

Following the RiskUE-LM1 approach, the mean damage grade, μ_D , of each building block was then determined through the convolution of its respective MMI and \bar{V}_I values:

$$\mu_D = 2.5 \cdot \left[1 + \tanh \left(\frac{MMI + 6.25 \cdot \bar{V}_I - 13.1}{2.3} \right) \right]$$

accompanied by the probability of occurrence, p_k per EMS-98 Damage Grades (**DG**), which is described by the cumulative beta distribution function, P_β , (Giovinazzi and Lagomarsino 2004):

The expected DGs are perceived as distinct variables, k , that range from 0 to 5 depending on the damage pattern: DG0-No damage, DG1-Slight damage, DG2-Moderate damage, DG3-Heavy damage, DG4-Very heavy damage, DG5-Total collapse.

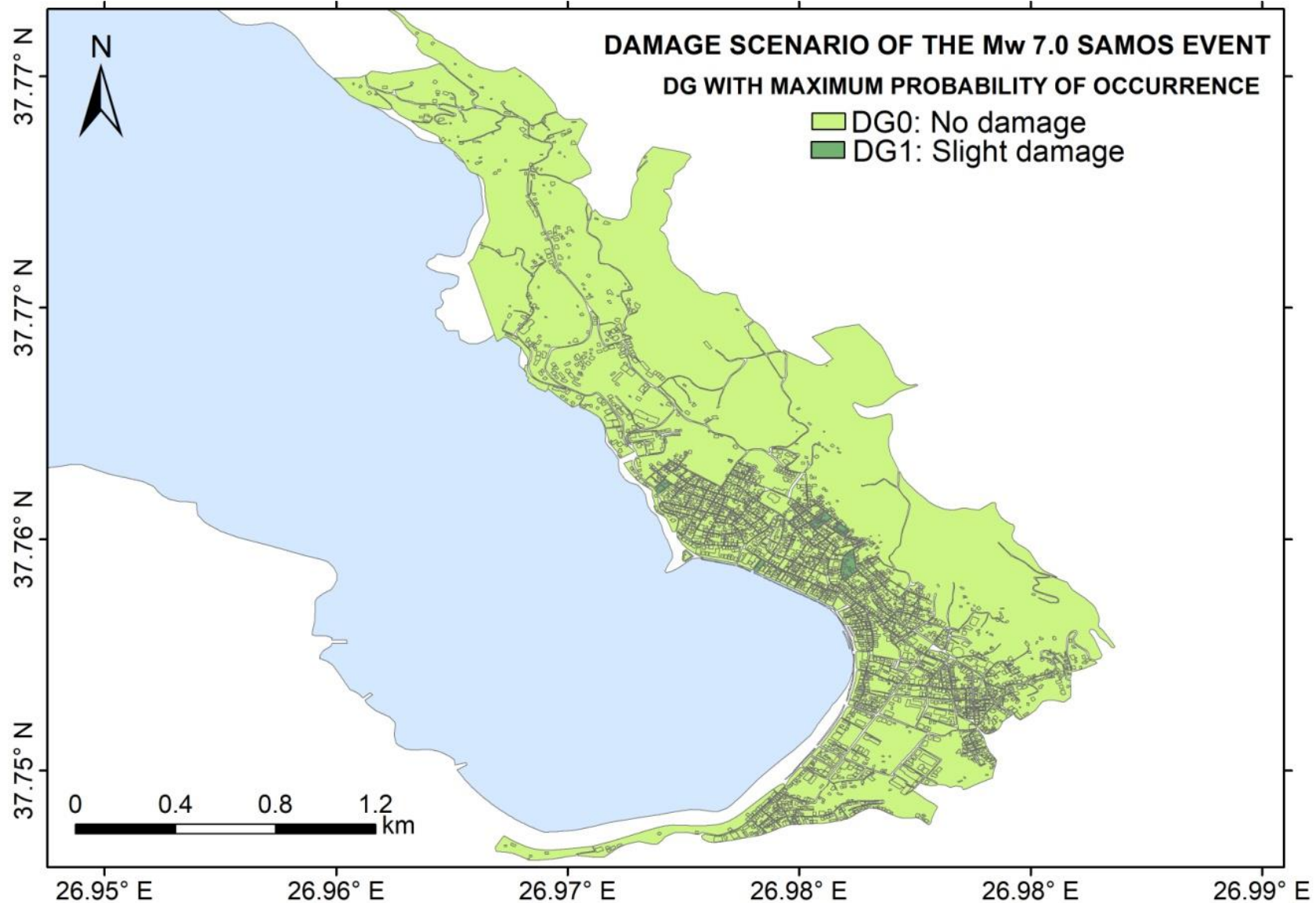
$$\mu_D = \sum_{k=0}^5 p_k \cdot k$$

$$p_k = P_\beta(k+1) - P_\beta(k)$$

Distribution of Damage Degree Levels of Maximum Probability of Occurrence

Although damage estimation in Vathy includes the possibility of all DGs, the highest degrees of damage; i.e. heavy to very heavy and total collapse, are negligible

Maximum Probability suggests no damage (DG0) to very limited slight damage (DG1) in the central, upper part of the town

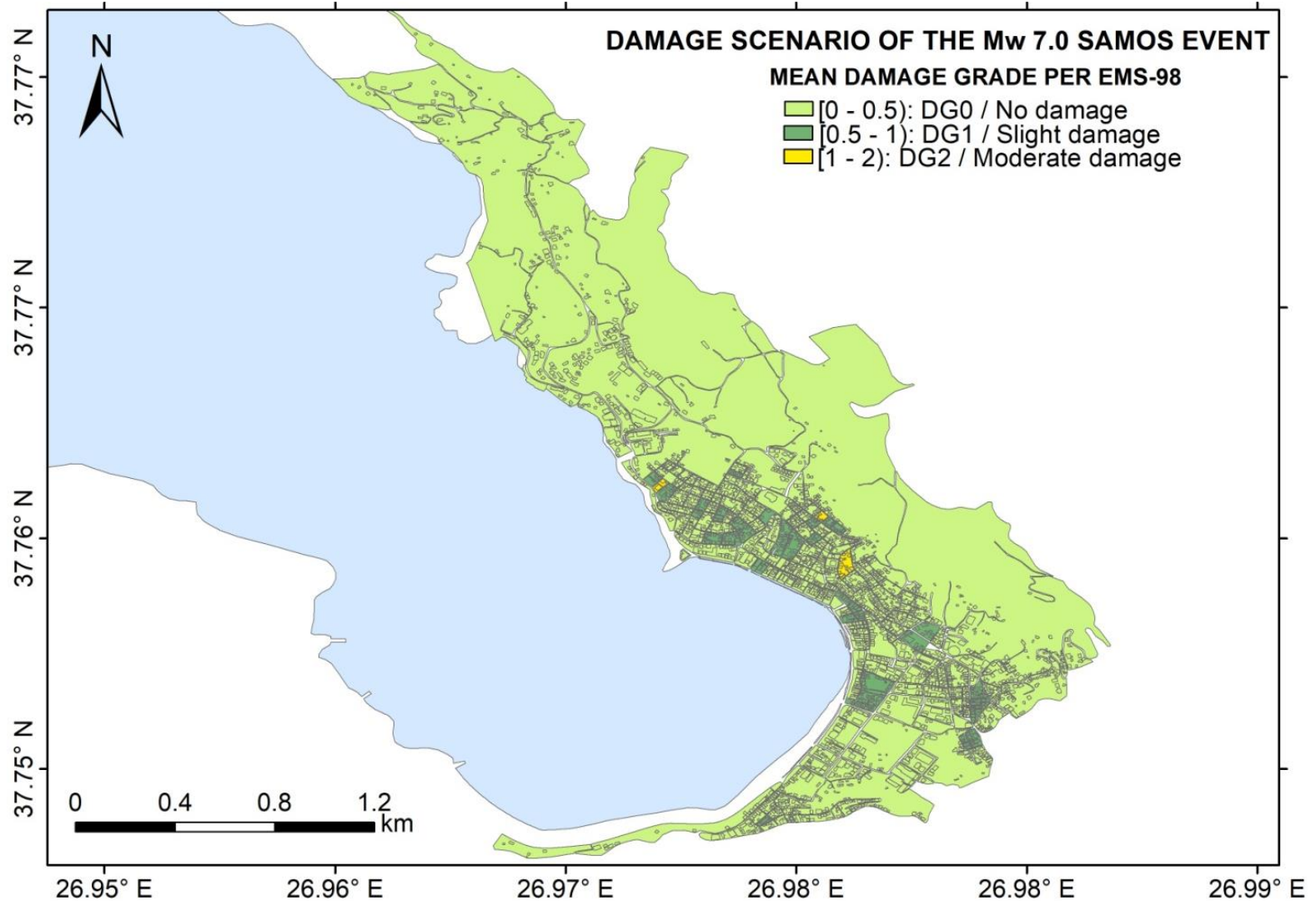


Distribution of Mean Damage Grade μD

Distribution of mean damage grade μD in the town of Vathy

The correlation between EMS-98 DG range is in accordance with Giannaraki et al., 2018 and Pomonis et al., 2014.

Other factors, not considered in our study, e.g. topographic effects, should be sought to explain the slightly higher damage levels that were observed in the southeastern part of Vathy (mainly to old, low-rise buildings and monumental structures)



Main Concluding remarks

- ❑ Higher synthetic PGAs were computed in the northern part of Vathy due to its closer proximity to the earthquake source and in the central part of the town due to the amplification of softer shallow soil formations. In general, however, synthetic PGAs do not surpass the levels set by the recorded PGAs at stations SMG1 and SAMA
- ❑ The predicted damage distribution in the town of Vathy verifies the observation that the building stock responded well, considered the magnitude of the event, with the majority of buildings remaining intact. Slight to moderate damage are derived for the central west of the seaside town, reflecting the exposure model
- ❑ The overall satisfactory structural performance of Vathy during the **M7.0** 2020 earthquake can be attributed to good construction characteristics; both low-rise URM and RC infrastructures. The predicted damage distribution is generally compatible with preliminary information in reconnaissance reports in Vathy. Additional effects, such as topographic, may be required to explain limited and localized deviations in predicted and observed damage

Perspectives

- Incorporate more detailed and solidified source models (including heterogeneous slip distributions) in forward simulations of strong ground motions in Vathy
- Incorporation of further geotechnical-geophysical data to better resolve the spatial variability of site effects
- Extend the application of the stochastic model beyond the near-fault area, e.g. in the town of Karlovasi in Samos and in the port of Chios Island, Greece

References:

- Atkinson G. M. and Boore D. M. (1995).** Ground-motion relations for eastern North America, *Bulletin of the Seismological Society of America*, Vol. 85, No. 1, pp. 17-30
- Atkinson G. and R. Mereu (1992).** The shape of ground motion attenuation curves in southeastern Canada, *Bulletin of the Seismological Society of America*, Vol. 82, No. 5, pp. 2014-2031.
- Boore DM (1984).** Use of seismoscope records to determine ML and peak velocities. *Bull Seismol Soc Am* 74(1):315–324
- Boore DM (1996).** SMSIM—Fortran programs for simulating ground motions from earthquakes: Version 1.0. U.S Department of the Interior. US Geological Survey Open-File Report 96-80-A and 96-80-B, pp 73
- Boore D.M. (2005).** SMSIM--Fortran programs for simulating ground motions from earthquakes: Version 2.3, U.S. Geological Survey, A revision of Open-File Report 96-80-A, pp. 17-23
- EPANTYK (2009).** Development of GIS software for the representation of the structural wealth of the municipalities of the country and of its structural vulnerability in buildings block level, YP.ES.A, H.D, KEDKE, TEE, pp. 39 (in Greek)
- GEER-069 Report (2020).** Seismological and Engineering Effects of the M 7.0 Samos Island (Aegean Sea) Earthquake, Geotechnical Extreme Events Reconnaissance Association, <https://doi.10.18118/G6H088>
- Giannaraki G., I. Kassaras, Z. Roumelioti, D. Kazantzidou–Firtinidou, A. Ganas (2018).** Deterministic seismic risk assessment in the city of Aigion (W. Corinth Gulf, Greece) and juxtaposition with real damage due to the 1995 Mw6.4 earthquake, *Bulletin of Earthquake Engineering*, Springer Nature B.V., pp. 1–32
- Giovinazzi S, Lagomarsino S (2004).** A macroseismic method for the vulnerability assessment of buildings. In: *Proceedings of the 13th WCEE*, Vancouver, BC, Canada, August 1–6, paper No 896
- Hatzidimitriou P. M. (1993).** Attenuation of coda waves in northern Greece, *Pageoph*. Vol. 140, pp. 63-78.
- Hatzidimitriou P. M. (1995).** S-wave attenuation in the crust in northern Greece, *Bulletin of the Seismological Society of America*, Vol. 85, pp. 1381-1387
- Margaris BN, Boore DM (1998).** Determination of $\Delta\sigma$ and κ_0 from response spectra of large earthquakes in Greece. *Bull Seismol Soc Am* 88(1):170–182
- Pitilakis K., Riga E., Anastasiadis A., (2019).** Towards the revision of EC8: Proposal for an alternative site classification scheme and associated site amplification factors, 4th Panhellenic Conference on Seismic Engineering and Seismology, Athens-Greece
- Plicka, V., Gallovič, F., Zahradník, J., Serpetsidaki, A., Sokos, E., Vavlas, N. and A. Kiratzi (2021).** The 2020 Samos (Aegean Sea) M7 earthquake: a normal fault with rupture directivity and near surface slip explaining the tsunami generation and coastal uplift, submitted.
- Pomonis A., Gaspari M., Karababa F.S. (2014).** Seismic vulnerability assessment for buildings in Greece based on observed damage data sets, *Bollettino di Geofisica Teorica ed Applicata*, Vol. 55, N. 2, pp. 501-534.
- Stewart J.P., Klimis N., Savvaidis A., Theodoulidis N., Zargli E., Athanasopoulos G., Pelekis P., Mylonakis G., and Margaris B. (2014).** Compilation of a Local V_s Profile Database and Its Application for Inference of V_{s30} from Geologic- and Terrain-Based Proxies, *Bulletin of the Seismological Society of America*, Vol. 104, No. 6, pp. 1–15, doi: 10.1785/0120130331
- Tselentis G-A, Danciu L (2008).** Empirical relationships between modified Mercalli intensity and engineering ground-motion parameters in Greece. *Bull Seismol Soc Am* 98(4):1863–1875
- Wells DL, Coppersmith KJ (1994).** New empirical relationships among magnitude, rupture length, rupture width, rupture area, and surface displacement. *Bull Seismol Soc Am* 84(4):974–1002

The Samos Mw6.9 event: Damage investigation in the town of Vathy incorporating a stochastic finite-fault source with site and structural information

Georgia Giannaraki^{1,2}, Zafeiria Roumelioti¹, and Nikolaos S. Melis²

¹University Of Patras, Department Of Geology, Patras-Greece

²National Observatory Of Athens, Institute Of Geodynamics, Athens-Greece

THANK YOU